This is a “preproof” accepted article for *Mineralogical Magazine*.

This version may be subject to change during the production process.

10.1180/mgm.2024.89

Selenolaurite, $RuSe_2$, a new mineral from the Ingul gold placer, South Urals, Russia

Belogub E.V.[1,2], Britvin S.N.[2,3], Shilovskikh V.V.[2], Pautov L.A.[4], Kotlyarov V.A.[1], Krzhizhanovskaya M.G.[2], Novoselov K. A.[1], Zaykova E.V.[1], Blinov I. A.[1]

[1] South Urals Federal Research Center of Mineralogy and Geoecology, Urals Branch of Russian Academy of Science, Miass, 456317, Russia

[2] Saint-Petersburg State University, Universitetskaya Nab. 7/9, Saint Petersburg, 199034, Russia

[3] Nanomaterials Research Center, Kola Science Center of the Russian Academy of Sciences, Fersman Str. 14, 184209 Apatity, Russia

[4] Fersman Mineralogical Museum, Russian Academy of Sciences, Leninsky ave. 18-2, Moscow, 115162, Russia

*E-mail: belogub_e@yahoo.com

Abstract

Selenolaurite, ideally $RuSe_2$, is a new mineral, the first natural ruthenium selenide. It was discovered in the assemblage with the Se-bearing moncheite, that both form xenomorphic inclusion in the aggregate of crystals of the Os-Ir-Ru minerals at the Ingul gold placer, Urals, Russia. Also mineral with selenolaurite composition was found as euhedral inclusion within grains of Pt-Fe alloy with isoferroplatinum composition at the Kazan gold placer. These placers situate at

https://doi.org/10.1180/mgm.2024.89 Published online by Cambridge University Press

the Chelyabinsk district, South Urals, Russia. The selenolaurite from Ingul placer forms interstitial grains with maximal size of section of 0.05-0.1 mm. Crystals of the selenolaurite from Kazan placer reach 20 μm in size. Selenolaurite is gray with metallic luster, isotropic. Reflectance values [R_{max}/R_{min} (%) for COM approved wavelengths (nm)]: 45.8(470), 44.3(546), 43.8(589), 43.1(650). Chemical composition of the holotype from Ingul placer corresponds to the empirical formula $(Ru_{0.99}Ir_{0.05})_{\Sigma 1.04}(Se_{1.92}Te_{0.03}S_{0.01})_{\Sigma 1.96}$. Selenolaurite is selenium-dominant analogue of laurite, RuS_2 with pyrite-type structure. It is cubic, space group $Pa\bar{3}$, a 5.9424 (2) Å, V 209.84 (2) $Å^3$, Z 4, $D_{calc.}$ 8.415 $g \cdot cm^{-3}$ (calculated on the basis of empirical formula and unit-cell parameters refined by Rietveld method). The crystal structure has been refined from the powder data to R_B = 0.0067.

The strongest lines of the X-ray powder diffraction pattern [d(Å), (I), (hkl)] are: 3.434(41)(111), 2.973(90)(200), 2.6580(100)(210), 2.4264(84)(211), 1.7913(87)(311). The possible sources of a Ru-Se mineralization at South Urals are ophiolitic ultramafic rocks enriched in Ru and depleted with sulfur.

Introduction

Ruthenium (Ru) is an important element widely used in modern technologies, mostly, for wear-resistant electrical contacts and thick-film resistors and, to a lesser degree, as a chemistry catalyst and extreme ultraviolet photomasks (Greenwood and Earnshaw, 1997). Ruthenium could also be used in anticancer therapy (Clarke, 2003). Ruthenium is produced as a by-product of extraction of Pt and other platinum group elements (PGEs).

Ruthenium similarly to other PGEs is very rare. Its average crustal abundance is 7.1 ppb (Lorand and Laguet, 2016). Ophiolite-associated chromitites are characterized by a relatively higher Ru content in comparison with chondrite (O'Driscoll and Gonzalez-Jimenez, 2016 and reference therein). Native metals of the Ir–Os–Ru system and sulfides of the laurite–erlichmanite series are the one of the main mineral forms of Ru in chromitites and ophiolitic ultramafic rocks (O'Driscoll and González-Jiménez, 2016). Ruthenium-dominate minerals are very few among PGMs and rare. This is the 7th Ru-dominant PGMs (including native Ru).

https://doi.org/10.1180/mgm.2024.89 Published online by Cambridge University Press

The average crustal abundance of Se is $5*10^{-6}$ wt. % (~50 ppb (Ovchinnikov 1990). The Se content of mantle peridotites varies from <1 ng/g^{-1} (ppb) to 130 ppb (Lorand and Laguet, 2016). Selenium predominantly accumulates in a sulfide melt in comparison to silicate one (a ratio of Se content in sulfide melt/silicate melt is $3*10^{2}$, Pattern et al., 2013 and reference therein). Accordingly, Se in igneous ultramafic rocks is associated with sulfides of base metals, which crystallized because liquation of sulfide melt from silicate and oxide melt due to affinity selenium with sulphur or postmagmatic fluid alteration (Lorand and Laguet, 2016). Due to different geochemical behavior, Ru and Se are rarely encountered during geological history.

In general, the PGE selenides are sparse compared to sulfides and tellurides. No selenides are mentioned in a well-known review of O'Driscoll and González-Jiménez (2016) in contrast to abundant data on tellurides, bismuthides and germanides. The Se content of more common platinum group minerals (PGMs) is also not discussed. No special attention for selenides has been paid in a recent review about placer (Cabri et al., 2022 and reference therein) and chromitite from different types of ultramaphic rocks (Zaccarini et al., 2018, 2022; Stepanov et al., 2020). Seventeen PGE selenides, however, are currently known from various localities worldwide (e.g., Johan et al., 1970; Davis et al., 1977; Jebwab et al. 1992; Cook et al. 1994; Polekhovskiy et al. 1997; Paar et al., 1998; Roberts et al., 2002; Vymazalová et al., 2012; Zaykov et al., 2017; Barkov et al., 2017, 2021; Krivovichev, 2021; Belogub et al., 2023). Selenium has been reported as a trace element in the outer rim of platinum-palladium grains from Corrego Bom Sucesso, Brazil, where the authors attribute selenium contamination to biofilms (Reith et al., 2016).

A Ru selenide, which is similar to selenolaurite in composition, was previously described in a gold-bearing placer of the Kundus River (Tyva Republic, Russia) (Zaykov et al., 2014). This selenide forms inclusions in native osmium up to 40 μm in size. The Se content of up to 5.93 wt. % was detected in minerals of the laurite–erlichmanite series from the inclusions in isoferroplatinum grains of the Kazan placer (Chelyabinsk district, Russia) (Belogub et al. 2019, Zaykova et al., 2020). The Ru selenide in assemblage with native osmium and clinochlore was also described as joint inclusion in magnesiochromite from the lode chromitites of the Pados-Tundra complex (Kola Peninsula, Russia) (Barkov et al., 2017).

https://doi.org/10.1180/mgm.2024.89 Published online by Cambridge University Press

This article describes a new mineral selenolaurite, which was approved by the Commission on New Minerals, Nomenclature and Classification of the International Mineralogical Association (no. 2020-027), and discus its condition of formation. Selenolaurite was discovered during routine mineralogical study of a heavy concentrate of the Ingul placer carried out by Viktor Zaykov (1938–2017). A holotype specimen of selenolaurite is deposited in the Natural Museum of the Ilmeny State Reserve (registration no. 920/geo840, Miass, Chelyabinsk district, 456317, Russia). Recently, we also found Se-dominant laurite as an inclusion in an isoferroplatinum grain from the Kazan gold placer. Selenolaurite is named as a Se-dominant analogue of laurite.

Material and Methods

Heavy concentrates enriched in Pt were given to V.V. Zaykov by N.P. Zemlyanskiy (Ingul Cooperative). The sample was collected in an open pit of the Ingul gold placer in 2016. Additional three samples from this placer were provided by N.P. Zemlyanskiy in 2021 for the refinement of mineral composition of the placer.

The chemical composition of selenolaurite was determined using a REMMA 2M scanning electron microscope (SEM) equipped with an Oxford Link energy-dispersive spectrometer (EDS) at an accelerating voltage of 20 kV, a beam current of 6 nA, and a beam diameter of 2 μm. The reference materials included metallic Rh, Pt, Os, Ir, Ru, Pd, Au, and Ag for corresponding metals, chalcopyrite (S, Fe, Cu), CdSe and Bi_2Se_3 (Se) (a set of standards NERMA.GEOL.25.10.74, Kyiv, 2005). Selenolaurite was also analyzed on a Tescan Vega 3 SBU SEM equipped with an Oxford Instruments, X-act EDS at an accelerating voltage of 20 kV and a beam current of 200–300 pA in a spot mode. The energy-dispersive (ED) spectra were acquired, processed and quantified in the Inca 5.02 software. The detection limit was reported to be no worse than 0.3 wt %. The EDS was calibrated following the quant optimization procedure on pure Co before and after analysis and the beam current drift was less than 1 %. Metallic Os, Rh, Pt, Ir, Ru, Pd for respective metals, pyrite (S, Fe), CoSe and Bi_2Se_3 (Se) and PbTe (Te), Se), set of standards NERMA. Kyiv, 2005, were used as reference materials (South Urals Federal Research Center of Mineralogy and Geoecology) Also chemical composition of the selenolaurite was analysed using electron

https://doi.org/10.1180/mgm.2024.89 Published online by Cambridge University Press

microprobe JEOL JCXA-733 with wave dispersive spectrometer (WDS), WDS (Fersman Mineralogical Museum); using an acceleration voltage = 20 kV; beam current = 20 nA; beam diameter = 2 μm, reference materials metallic Rh, Pt, Ir, Ru, Pd for respective metals, pyrite (S, Fe), Bi_2Se_3 (Se) and HgTe (Te). The formulas were recalculated to three atoms for the laurite–selenolaurite series and moncheite and one atom for the Os–Ir–Ru alloys.

Element distribution maps and additional data on chemical composition were obtained on a Hitachi S-3400N SEM equipped with an Oxford Instruments X-Max 20 EDS at an accelerating voltage of 10 kV and a beam current of 1 nA to increase the locality of the ED analysis at the GEOMODEL Resource Center (Saint Petersburg State University (SPbU), St Petersburg, Russia). The spectrometer was calibrated against pure Os, Rh, Pt, Ir, Ru, Pd, Se, Te and pyrite (for S) (Micro-Analysis Consultants Ltd (MAC) standards).

The electron back-scattered diffraction (EBSD) maps were obtained using an Oxford Instruments HKL NordlysNano detector mounted on the abovementioned SEM (GEOMODEL Resource Center, Scientific Park, SPbU). The acquisition conditions were as follows: 30 kV and 1.5 nA, exposition 0.5 s per pattern, averaging 3–5 images (when mapping) or 20 images (to obtain individual high quality patterns). All the images were subsequently processed using Oxford AzTec and Channel5 software packages from Oxford Instruments. The structural data on laurite crystal (Sutarno et al., 1967) were used for the comparison and those of native osmium (Levi and Picot, 1961) and shuangfengite (ICSD 33934) were used as references for EBSD mapping. Shuangfengite $IrTe_2$ has the same trigonal structure as moncheite $PtTe_2$ (space group $P\bar{3}m1$). The lattice parameters *a* and *c* of shuangfengite and moncheite differ by 3 and 2%, respectively, therefore, given the sensitivity of EBSD for unit cell values not better than 10%, structural data on shuangfengite was used as a reference for moncheite mapping. The orientation of individual selenolaurite crystals is shown in Euler color schemes, pole figures and orientation distribution density heatmaps (Mason and Schuh, 2009). To obtain a mechanically undistorted surface, a sample for the EBSD analysis was treated with a direct beam of Ar plasma on an Oxford Instruments Ionfab300 etcher at an exposition of 10 min, an angle of 45°, an accelerating voltage of 500 V, a current of 200 mA, and a beam diameter of 10 cm (Nanophotonics Resource Center, Scientific Park, SPbU).

X-ray powder diffraction data were collected for material extracted from the polish section which was analysed using WDS on a Rigaku RAXIS Rapid II diffractometer (curved (cylindrical) imaging plate (r = 127.4 mm)) using Co*K*α-radiation (λ = 1.79021 Å), a rotating anode (40 kV, 15 mA) with microfocus optics, Debye-Scherrer geometry, *r* = 127.4 mm, and an exposure 30 min. The calculated *d*-spacings and intensities were obtained in Stoe WinXPOW v. 1.28 program based on the unit-cell parameters and atomic coordinates refined by Rietveld method. The Rietveld refinement of the crystal structure was carried out in Bruker TOPAS v. 5.0 software with R_B = 0.0067. No single-crystal X-ray studies were performed because of lackingof a sufficient amount of the material.

Reflectance data for selenolaurite were obtained on a LOMO MSP-R microscope–spectrophotometer equipped with a PEI “R928” spectrophotometric device (Hamamatsu, Japan) at the South Urals Federal Research Center of Mineralogy and Geoecology, Miass, Russia. The reflectance spectra for a 420–700-nm range were measured in air using an objective of x40 with a numerical aperture of 0.65: a photometric diaphragm of 0.3 mm, a size of an analyzing area of 0.007 mm, diffraction grating of 600 grooves/mm, a spectral interval of 6 nm, a voltage for PEI of 450 V, and elemental silicon as a standard..

Geological background

Selenolaurite was first found in a heavy concentrate of the Ingul gold placer. The Ingul placer (55°04'49" N, 60°34'11" E) belongs to the Nepryakhino gold placer zone and is situated ~75 km SW of Chelyabinsk (Figure 1) and 8 km ENE of the Nepryakhino village in Chelyabinsk district (Figure 2a). The Nepryakhino gold placer zone is longitudinally extended concordant with a general strike of the Uralian fold structure. The placer zone includes proluvial and alluvial placers (unpublished report of geological survey of “UralNedra”). The current topography of the territory is plain. The Nepryakhino placer zone is separated from the zone of the Main Ural Fault with most gold placers of Miass River by metasediments of the Ilmeno-Vishnegorsk zone (Figure 1), forming positive relief forms. The Upper Miocene to Pleistocene placer is localized in the valley of the Ingul River, a right tributary of the Miass River (Zaykov et al., 2017). The length of the placer reaches 6.5

https://doi.org/10.1180/mgm.2024.89 Published online by Cambridge University Press

km at a width of 20–40 m. The thickness of the peat and sand layers is 3.5 and 0.5–1.2 m, respectively. The placer has intermittently been exploited since 1900. The Au content varied from 0.3 to 1.2 g/m^3 (unpublished report of geological survey of “UralNedra”). There is no information on the PGE content of the placer but the findings of PGMs are known.

A few small primary gold deposits and occurrences have been explored in the Nepryakhino gold placer zone, but similar objects are unknown near the Ingul placer (Figure 1b). The deposits mainly include gold-bearing quartz veins and rare disseminated quartz–sulphide zones.

Some small unnamed fully serpentinized gabbro–dunite–harzburgite massifs of the Ordovician Chebarkul–Katsbakh complex are situated to the west of the Ingul placer. All of them are covered by Quaternary sediments. No data on the PGE content or the presence of the PGMs are available for these massifs.

Also we found selenolaurite in Pt-Fe alloy with isoferroplatinum composition during reexamination of the heavy concentrate of the Kazan gold placer (South Urals), which is localized in the Bredy erosion-structural depression of the Cenomanian – Upper Pleistocenene age. It is located at the confluence of the Karagayly-Ayat and Kamyshly-Ayat rivers, but there are no permanent watercourses in close proximity to the placer. The raft is represented by karsted Lower Carboniferous limestone. More detail geological and geomorphological explanation of the Kazan placer was clarified previously (Belogub et al., 2022).

https://doi.org/10.1180/mgm.2024.89 Published online by Cambridge University Press

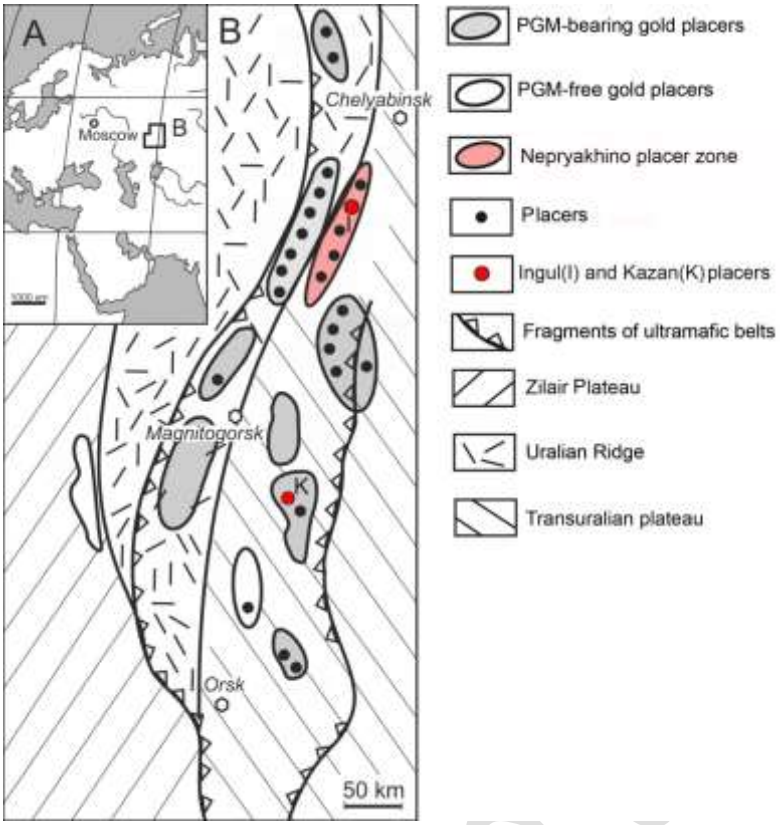

Fig. 1. Geographic setting of the South Urals (a) and location of main placer zones and placers with data on placer mineral assemblages (b), simplified after (Zaykov et al., 2017).

https://doi.org/10.1180/mgm.2024.89 Published online by Cambridge University Press

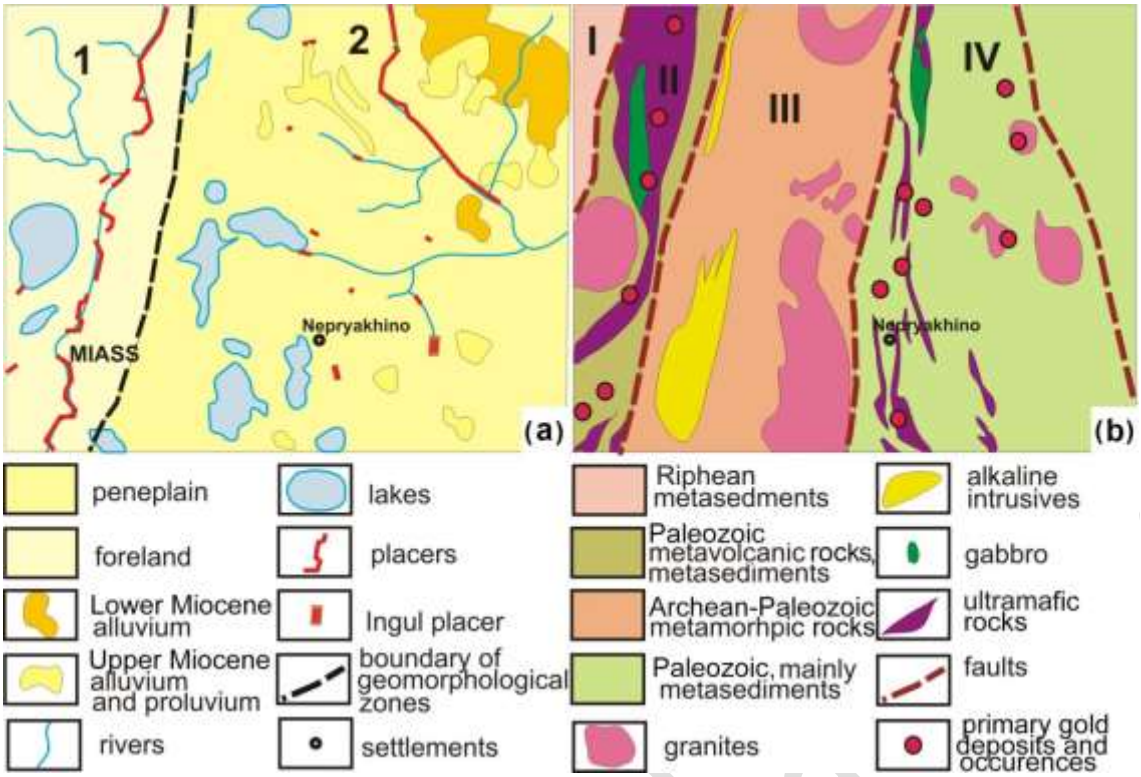

Fig. 2. Position of the Ingul placer in the Nepryakhino placer zone in the geomorphological sketch (a) and geological map of the pre-Cenozoic basement (b), simplified after (unpublished materials of Uralnedra). Morphological structures: 1, Miass foreland; 2, Bayramgulovo uplifted peneplain. Metallogenic zones: I, West Uralian; II, Main Urals Fault; III, Ilmeno-Vishnevogorsk; IV, East Uralian.

Assemblage and morphology of selenolaurite

Ingul placer

The heavy concentrate of the Ingul gold placer includes Os–Ru–Ir alloys, Se-bearing moncheite, chromite, thorite, tantalite, magnetite, ilmenite, and native gold (Zaykov et al., 2017; Rassomakhin and Zaykov, 2017), as well as Fe and Mn oxyhydroxides, amphibole, hematite, almandine, pyrite (including that with inclusions of Ag and Bi tellurides), limonite pseudomorphoses after pyrite, arsenopyrite, rutile, molybdenite, zircon, tourmaline, barite, monazite, and kyanite (our data). Quartz, albite, orthoclase, microcline, talc, muscovite, kaolinite, and minerals of the serpentine group are the gangue minerals of the alluvium.

https://doi.org/10.1180/mgm.2024.89 Published online by Cambridge University Press

Native gold is a main noble metal mineral. It is slightly rounded. The native gold grains are locally euhedral and have the footprints of other minerals, which is evidence of the proximity of a primary source. The fineness of native gold varies from ~850 to 950‰.

The size of the studied PGMs grains was typically up to 0.5 mm, locally, reaching 1–2 mm. The chemical composition of 139 PGM grains shows a Ru trend of the composition of the Os–Ru–Ir alloys (Rassomakhin and Zaykov, 2017). No native Pt minerals were found in the Ingul placer. Selenolaurite forms anhedral interstitial grains between the aggregates of platy native osmium crystals up to 0.3 mm in size. The maximal size of sections of selenolaurite is 0.05–0.1 mm. Selenolaurite is closely intergrown with Se-bearing Pd- and Bi-free moncheite (Fig. 3). The chemical composition of the Os–Ir–Ru alloy and moncheite are shown in Tables 1 and 2, respectively. According to the EBSD patterns fitting and mapping data, the structure of the moncheite phase is similar to shuangfengite $IrTe_2$ with a mean angle deviation MAD less than 1° (0.48° for a selected high-resolution EBSD pattern) on the basis of 12 bands detection.

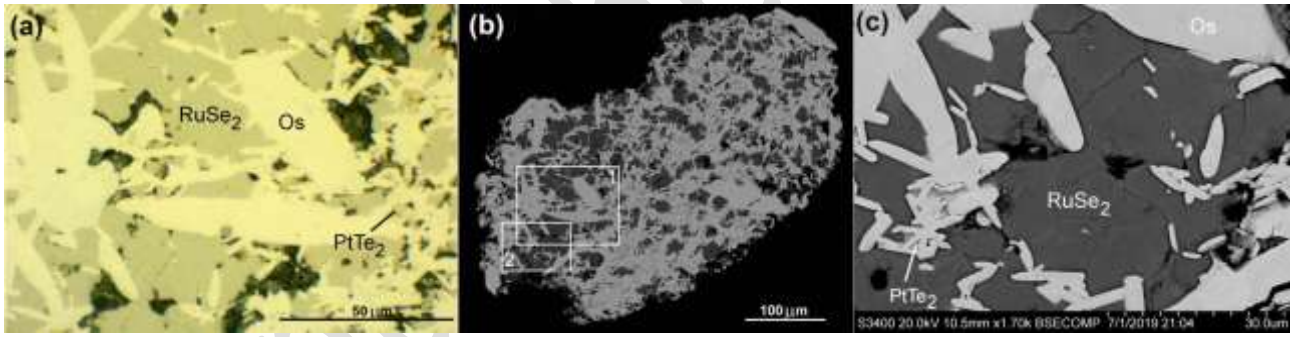

Figure 3. Interstitial holotype selenolaurite ($RuSe_2$) and Se-bearing moncheite between the aggregates of native osmium crystals (Os), Ingul placer: (a) reflected light (oil immersion); (b) BSE image of the grain with the aggregate of platy native osmium crystals and areas of the reflected light image (1) and detailed BSE image (2); (c) BSE image of anhedral selenolaurite aggregate between native osmium crystals.

Kazan placer

Selenolaurite and Se-bearing laurite from the Kazan placer form inclusions up to 20 μm in size in Pt_3Fe grains. The Pd- and Cu-bearing native gold, native osmium and Cr-enriched

https://doi.org/10.1180/mgm.2024.89 Published online by Cambridge University Press

magnetite also occur as inclusions in coarser Pt_3Fe grains (Fig. 4). The euhedral Se-bearing laurite intergrowths with cooperite (Fig. 4a).

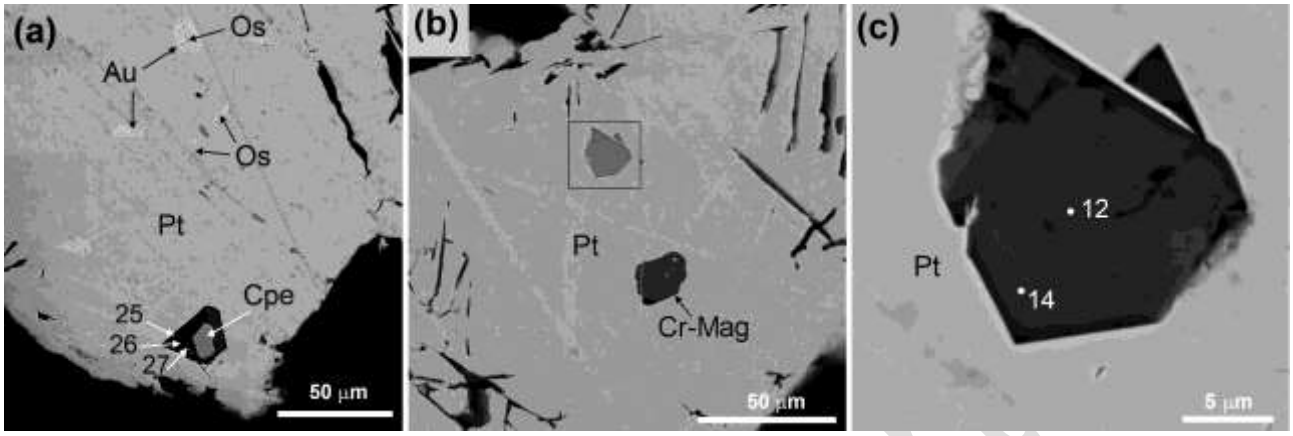

Figure 4. Inclusions of Se-bearing laurite (a, points 25, 26, 27) and selenolaurite (b, c, points 12, 13) in Pt_3Fe, the Kazan placer. Cpe, cooperite; Cr-Mag, Cr-enriched magnetite; Au, native gold; Os, native osmium; Pt, Pt_3Fe.

Table 1. Chemical composition of Os–Ir–Ru alloy crystals with interstitial selenolaurite (wt. %

No	Ru	Os	Ir	Pt	Total	Calculated formula
1	0.96	71.89	27.02	0.00	99.87	$Os_{0.72}Ir_{0.27}Ru_{0.02}$
2	1.53	72.39	25.24	0.13	99.29	$Os_{0.72}Ir_{0.25}Ru_{0.03}$
3	1.19	75.76	22.26	0.00	99.21	$Os_{0.76}Ir_{0.22}Ru_{0.02}$

Note. Here and in Table 3, dash is below detection limit. EDS, REMMA 2M.

https://doi.org/10.1180/mgm.2024.89 Published online by Cambridge University Press

Table 2. Chemical composition of moncheite associated with selenolaurite (wt. %)

No	Pt	Ir	Te	Se	Total	Calculated formula
1	34.40	10.69	47.17	6.80	99.05	$(Pt_{0.77}Ir_{0.24})_{\Sigma 1.01}(Te_{1.61}Se_{0.38})_{\Sigma 1.99}$
2	36.15	10.57	45.45	7.05	99.22	$(Pt_{0.81}Ir_{0.24})_{\Sigma 1.05}(Te_{1.56}Se_{0.39})_{\Sigma 1.95}$
3	36.17	10.11	45.72	7.18	99.18	$(Pt_{0.81}Ir_{0.23})_{\Sigma 1.04}(Te_{1.56}Se_{0.40})_{\Sigma 1.96}$

Note. EDS, REMMA-2M

Chemical composition of selenolaurite

The chemical composition of selenolaurite is shown in Table 3. The average empirical formula of the holotype calculated on the basis of three atoms per formula unit is $(Ru_{0.99}Ir_{0.05})_{\Sigma 1.04}(Se_{1.92}Te_{0.03}S_{0.01})_{\Sigma 1.96}$. The simplified formula is $RuSe_2$. The ideal formula $RuSe_2$ requires (wt. %) 39.05 Ru and 60.95 Se. Selenolaurite from the Ingul placer contains some Ir (3.28-5.50 wt.%), Te (0.61-1.93 wt. %) and S (<LOD-0.18 wt .%). In contrast, selenolaurite and Se-bearing laurite of the Kazan placer is characterized by the presence of Os (0.71-27.50 wt. %), Ir (nill-5.88 wt. %), Rh (5.04-15.65 wt. %), Pt (0.39-4.83 wt. %) and As (nill-9.63 wt. %) and the absence of Te (Table 3).

According to microgeochemical mapping, selenolaurite from the Ingul placer is the main concentrator of Ru and Se in the studied aggregate (Fig. 5). In contrast, the composition of selenolaurite from the Kazan placer varies even within one grain (Fig. 4, Table 3 analyses nos. 12-13 and 25-27).

https://doi.org/10.1180/mgm.2024.89 Published online by Cambridge University Press

Table 3. Chemical composition of selenolaurite and Se-bearing laurite (wt. %)

No	Ru	Os	Ir	Rh	Pt	Fe	Se	S	As	Te	Total
1	38.07		3.28	0.20	-	-	57.52	0.18	-	0.97	100.22
2	37.91		3.65	0.08	0.03	-	57.10	0.01	-	1.70	100.49
3	38.98		3.34	-	-	-	56.33	-	-	1.35	100.00
4	37.22		4.59	-	-	-	57.13	-	-	1.06	100.00
5	37.83		4.95	-	-	-	55.62	-	-	1.59	100.00
6	37.51		5.50	-	-	-	55.63	-	-	1.36	100.00
7	37.85		4.49	-	-	-	57.04	-	-	0.61	100.00
8	37.90		4.52	-	-	-	55.65	-	-	1.93	100.00
9	38.43		3.53	-	-	-	56.74	-	-	1.30	100.00
10	39.20		4.00	-	-	-	55.69	-	-	1.11	100.00
11	31.83	1.30	1.15	5.04	0.39	-	59.54	-	-	0.19	99.44
12	27.10	1.16	1.25	11.32	2.16	0.13	49.63	0.95	6.43	0.48	100.61
13	30.03	0.31	0.89	11.32	1.27	-	43.7	5.49	7.59	-	100.60
14	28.57	0.74	1.07	11.32	1.72	0.13	46.67	3.22	7.01	0.48	100.61
15	40.84	4.70	1.51	8.84	3.2	0.15	11.7	25.34	3.72	-	100.00
16	35.54	23.29	-	3.40	0.65	-	5.93	29.24	2.34	-	100.39
17	31.79	4.24	5.88	15.65	-	-	5.57	26.94	9.63	-	99.71

https://doi.org/10.1180/mgm.2024.89 Published online by Cambridge University Press

18	34.02	25.22	-	3.29	0.61	-	5.55	29.14	2.38	-	100.20
19	50.67	5.09	1.01	1.90	1.51	-	5.25	32.61	2.19	-	100.21
20	32.50	27.15	-	3.18	0.56	-	5.17	29.03	2.41	-	100.00
21	37.93	10.04	2.49	6.28	1.9	-	2.13	29.82	8.47	-	99.06
22	39.50	15.82	3.2	3.59	1.31	-	2.11	32.25	3.20	-	100.98
23	35.04	13.66	2.23	5.85	4.83	0.31	1.25	29.29	7.06	-	99.53
24	33.18	19.22	1.47	4.59	4.35	0.30	0.63	30.20	5.60	-	99.53
25	40.21	16.47	2.49	2.97	1.14	-	1.92	32.04	2.80	-	100.03
26	40.92	17.11	1.77	2.35	0.96	-	1.72	31.82	2.40	-	99.07
27	28.86	31.51	-	2.33	2.37	-	0.45	30.67	3.17	-	100.98

Calculated formula

1. $(Ru_{0.99}Ir_{0.05})_{\Sigma 1.04}(Se_{1.92}Te_{0.02}S_{0.02})_{\Sigma 1.96}$
2. $(Ru_{0.99}Ir_{0.05})_{\Sigma 1.04}(Se_{1.92}Te_{0.04})_{\Sigma 1.96}$
3. $(Ru_{1.03}Ir_{0.05})_{\Sigma 1.07}(Se_{1.90}Te_{0.03})_{\Sigma 1.93}$
4. $(Ru_{0.98}Ir_{0.07})_{\Sigma 1.05}(Se_{1.93}Te_{0.02})_{\Sigma 1.95}$
5. $(Ru_{1.00}Ir_{0.07})_{\Sigma 1.07}(Se_{1.93}Te_{0.02})_{\Sigma 1.93}$
6. $(Ru_{1.00}Ir_{0.08})_{\Sigma 1.08}(Se_{1.90}Te_{0.03})_{\Sigma 1.93}$
7. $(Ru_{1.00}Ir_{0.06})_{\Sigma 1.06}(Se_{1.93}Te_{0.01})_{\Sigma 1.94}$
8. $(Ru_{1.01}Ir_{0.06})_{\Sigma 1.07}(Se_{1.93}Te_{0.04})_{\Sigma 1.97}$
9. $(Ru_{1.01}Ir_{0.05})_{\Sigma 1.06}(Se_{1.91}Te_{0.03})_{\Sigma 1.94}$
10. $(Ru_{1.04}Ir_{0.06})_{\Sigma 1.10}(Se_{1.89}Te_{0.01})_{\Sigma 1.90}$

https://doi.org/10.1180/mgm.2024.89 Published online by Cambridge University Press

11. $(Ru_{0.83}Rh_{0.13}Os_{0.02}Ir_{0.02}Pt_{0.01})_{\Sigma\ 1.01}Se_{\Sigma\ 1.99}$

12.d $(Ru_{0.70}Rh_{0.29}Pt_{0.03}Os_{0.02}Ir_{0.02}\ Fe_{0.01})_{\Sigma\ 1.05}(Se_{1.64}As_{0.22}S_{0.08}Te_{0.01})_{\Sigma\ 1.95}$

13.c $(Ru_{0.72}Rh_{0.26}\ Pt_{0.02}Ir_{0.01})_{\Sigma\ 1.01}(Se_{1.33}S_{0.41}As_{0.24})_{\Sigma\ 1.98}$

14. $(Ru_{0.71}Rh_{0.27}\ Pt_{0.02}Os_{0.01}Ir_{0.01}\ Fe_{0.01})_{\Sigma\ 1.03}(Se_{1.48}S_{0.25}As_{0.23}Te_{0.01})_{\Sigma\ 1.97}$

15. $(Ru_{0.79}Rh_{0.17}Os_{0.05}Pt_{0.03}Ir_{0.02}Fe_{0.01})_{\Sigma\ 1.06}(S_{1.55}Se_{0.29}As_{0.10})_{\Sigma\ 1.94}$

16. $(Ru_{0.69}Os_{0.24}Rh_{0.06}Pt_{0.01})_{\Sigma\ 1.00}(S_{1.79}As_{0.15}Se_{0.06})_{\Sigma\ 2.00}$

17. $(Ru_{0.61}Rh_{0.29}Os_{0.04}Ir_{0.06})_{\Sigma\ 1.00}(Se_{0.14}As_{0.25}S_{1.62})_{2.00}$

18. $(Ru_{0.67}Os_{0.26}Rh_{0.06}Pt_{0.01})_{\Sigma\ 1.00}(S_{1.80}As_{0.14}Se_{0.06})_{\Sigma\ 2.00}$

19. $(Ru_{0.90}Os_{0.05}Rh_{0.03}Ir_{0.01}Pt_{0.01})_{\Sigma\ 1.00}(S_{1.82}Se_{0.12}As_{0.05})_{\Sigma\ 2.00}$

20. $(Ru_{0.64}Os_{0.29}Rh_{0.06}Pt_{0.01})_{\Sigma\ 1.00}(S_{1.81}As_{0.13}Se_{0.06})_{\Sigma\ 2.00}$

21. $(Ru_{0.71}Rh_{0.12}Os_{0.10}Ir_{0.02}Pt_{0.02})_{\Sigma\ 0.97}(S_{1.76}As_{0.21}Se_{0.05})_{\Sigma\ 2.03}$

22. $(Ru_{0.73}Os_{0.16}Rh_{0.07}Ir_{0.03}Pt_{0.01})_{\Sigma\ 0.99}(S_{1.88}As_{0.08}Se_{0.05})_{\Sigma\ 2.01}$

23. $(Ru_{0.68}Os_{0.14}Rh_{0.11}Ir_{0.02}Pt_{0.05}\ Fe_{0.01})_{\Sigma\ 1.00}(S_{1.79}As_{0.18}Se_{0.03})_{\Sigma\ 2.00}$

24. $(Ru_{0.64}Os_{0.20}Rh_{0.09}Ir_{0.01}Pt_{0.04}Fe_{0.01})_{\Sigma\ 0.99}(S_{1.84}As_{0.15}Se_{0.02})_{\Sigma\ 2.01}$

25.h $(Ru_{0.75}Os_{0.16}Rh_{0.05}Ir_{0.02}Pt_{0.01})_{\Sigma\ 1.06}(S_{1.88}As_{0.07}Se_{0.05})_{\Sigma\ 2.00}$

26.g $(Ru_{0.77}Os_{0.17}Rh_{0.04}Pt_{0.03}Ir_{0.02})_{\Sigma\ 1.06}(S_{1.89}As_{0.06}Se_{0.04})_{\Sigma\ 1.99}$

27.f $(Ru_{0.57}Os_{0.33}Rh_{0.05}Ir_{0.02}Pt_{0.02})_{\Sigma\ 0.99}(S_{1.91}As_{0.08}Se_{0.01})_{\Sigma\ 2.00}$

Note. 1-10 – Ingul placer, 11-26 Kazan placer, analysis nos. 1, 2, WDS, JEOL JCXA-733; analysis Nos 3-10 EDS REMMA-2M, analysis Nos. 11-26 – EDS VEGA 3 TESCAN)

https://doi.org/10.1180/mgm.2024.89 Published online by Cambridge University Press

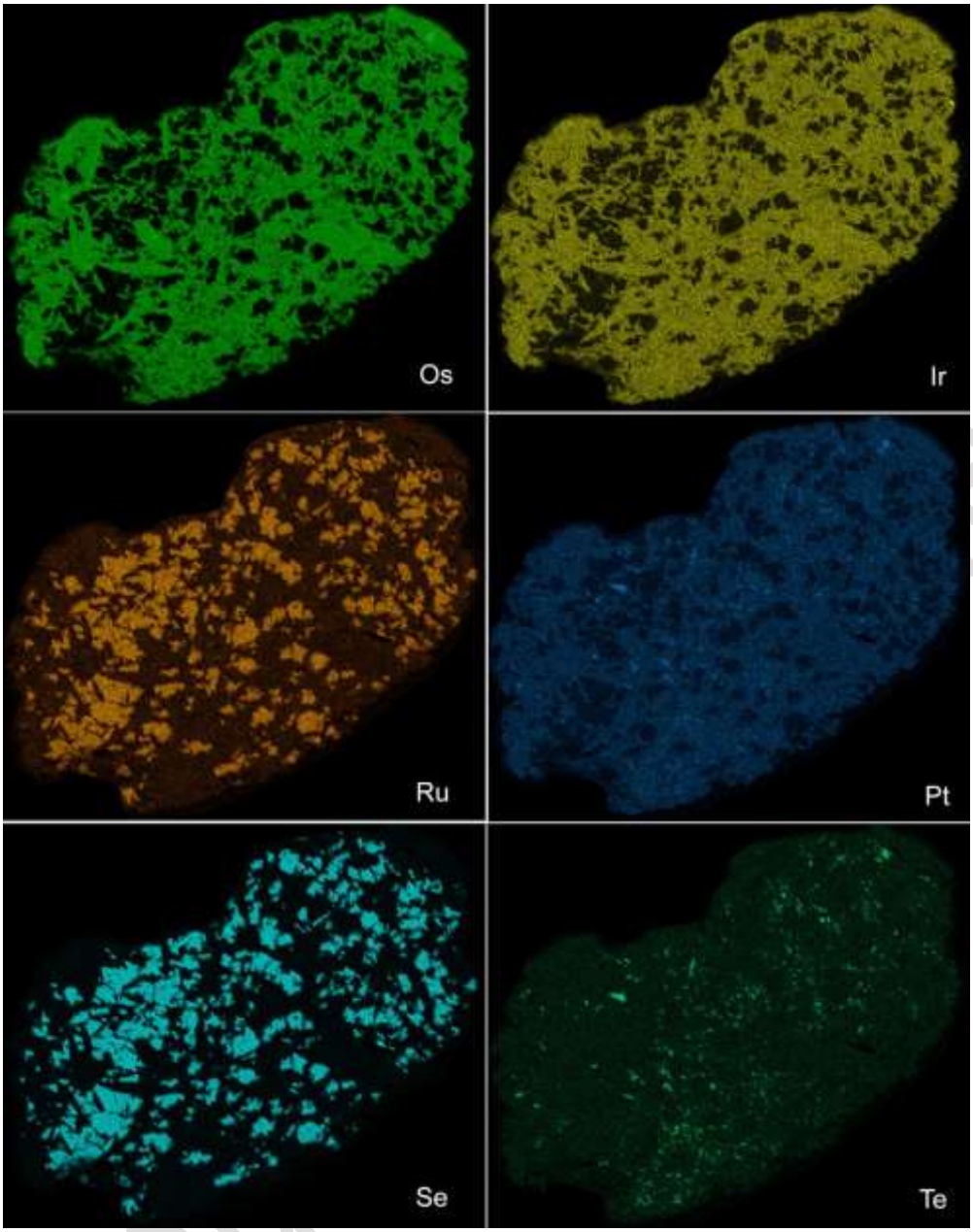

Figure 5. Elements distribution in the studied aggregate of native osmium, holotype selenolaurite and Se-bearing moncheite.

Physical properties of selenolaurite

Selenolaurite is opaque with a metallic lustre. It is nonmagnetic. The steak is black. The Mohs hardness is lower than that of native osmium (6–7) and higher than that of moncheite (2–3). Micro-indentation (Vickers hardness) could not reliably be measured due to intimate intergrowths with native osmium and moncheite. Selenolaurite is brittle; no cleavage and parting are observed. The density calculated on the basis of empirical formula and unit-cell parameters refined by Rietveld method is 8.415 $g \cdot cm^{-3}$. Selenolaurite is insoluble in cool concentrated HCl.

https://doi.org/10.1180/mgm.2024.89 Published online by Cambridge University Press

Selenolaurite is grey in reflected light. It has no bireflection, pleochroism, anisotropy and internal reflections. The reflectance values were measured for the selenolaurite holotype. The mean value of 4 measerements of different site is shown in Table 4. The reflectance level of selenolaurite is similar with that of laurite (Fig. 6). The reflectance spectrum is characterized by normal dispersion and a steep slope in the blue area with flattening in the yellow–red area in contrast to the spectrum of laurite, which has a more uniform slope. The reflectance and the spectrum shape of laurite varies depending on its chemical composition (Leonard and Desborough, 1969), therefore, the difference in the shape of the spectrum of selenolaurite from laurite is quite understandable.

Table 4. Mean reflectance values of selenolaurite

λ (nm)	*R*	λ(nm)	*R*
400	50.9	560	44.2
420	48.5	580	43.9
440	47.0	589 (COM)	43.8
460	46.1	600	43.7
470 (COM)	45.8	620	43.4
480	45.4	640	43.2
500	44.9	650 (COM)	43.1
520	44.6	660	43.0
540	44.4	680	42.7
546 (COM)	44.3	700	42.6

https://doi.org/10.1180/mgm.2024.89 Published online by Cambridge University Press

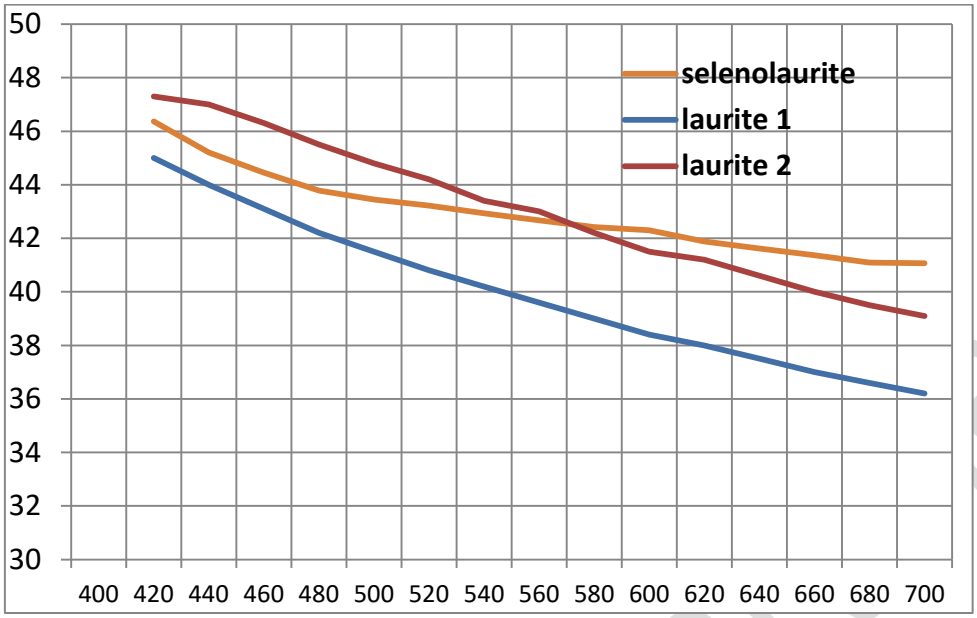

Figure 6. Reflection spectra of selenolaurite in comparison with laurite: laurite 1, data from (Roberts et al, 1990); laurite 2, data of M. Tarkian and H.-J. Bernhardt (1985) in (The quantitative…, 1986).

Structure of selenolaurite

The crystal structure of selenolaurite was refined by Rietveld method using starting parameters of synthetic $RuSe_2$ (Lutz et al., 1990). The powder sample was found to consist of 21 wt. % selenolaurite, 73 wt.% native osmium, and 6 wt.% moncheite (Fig. 7), therefore, several lines of selenolaurite are overlapped with the lines of metallic osmium (Table 5). The refined results are given in Table 6. Fractional atomic coordinates are provided in Table 7.

Selenolaurite have a pyrite-type structure. It crystallizes in a cubic system, space group $Pa\bar{3}$ (#205). The unit-cell parameters refined from X-ray powder diffraction data are as follows: a = 5.9424 (2) Å, V = 209.84 (2) Å^3, and Z = 4 (Table 6). The atomic coordinates are shown in Table 7.

https://doi.org/10.1180/mgm.2024.89 Published online by Cambridge University Press

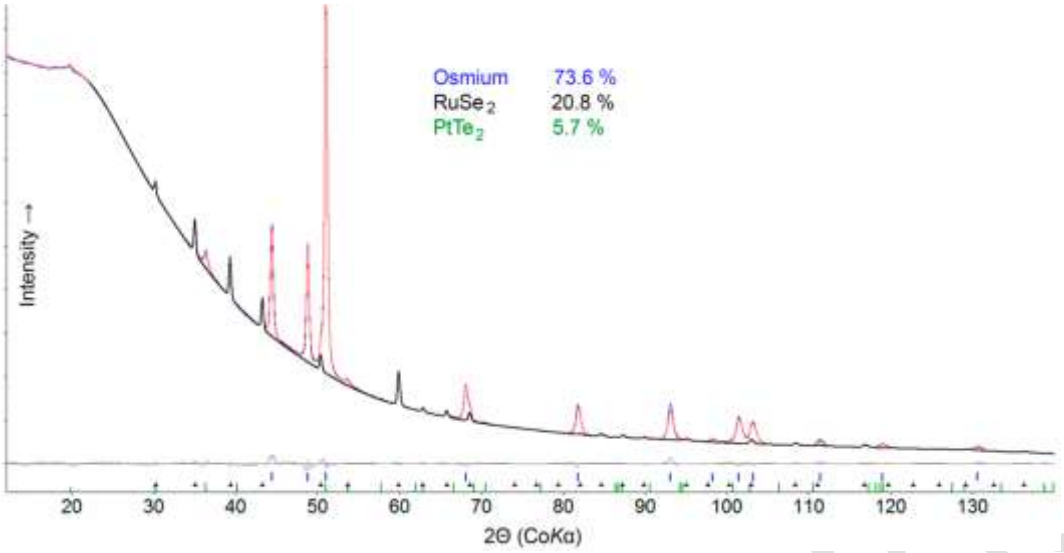

Figure 7. Rietveld refinement plot of a powder sample composed of selenolaurite, native osmium and moncheite. The black line highlights the calculated profile of selenolaurite

Table 5. X-ray powder diffraction data (*d* in Å) for selenolaurite*

I_{meas}	d_{meas}	I_{calc}	d_{calc}	*hkl*	I_{meas}	d_{meas}	I_{calc}	d_{calc}	*hkl*
41	3.434	26	3.431	111	4	1.2664	4	1.2669	332
90	2.973	80	2.971	200	7	1.2127	6	1.2130	422
100	2.6580	100	2.6575	210		x	3	1.1436	333
84	2.4264	76	2.4260	211			13	1.1436	511
	x	40	2.1010	220	6	1.1033	6	1.1035	342
87	1.7913	90	1.7917	311			2	1.1035	250
12	1.7152	11	1.7154	222		x	3	1.0849	251
18	1.6477	17	1.6481	230			2	1.0849	521
	x	10	1.5882	231	9	1.0503	12	1.0505	440
	x	15	1.5882	321	5	0.9902	4	0.9904	442
		1	1.4856	400	2	0.9771	2	0.9769	610
	x	3	1.3633	331	4	0.9638	1	0.9640	352
8	1.3284	4	1.3288	240			3	0.9640	532
		4	1.3288	420			2	0.9640	611
8	1.2965	9	1.2967	421					

Note. * x denotes the lines overlapped with reflections of metallic osmium.

https://doi.org/10.1180/mgm.2024.89 Published online by Cambridge University Press

Table 6. Rietveld refinement details for selenolaurite

Diffractometer	Rigaku RAXIS Rapid II (curved imaging plate)
Radiation	Co$K\alpha_1$ / Co$K\alpha_2$
μ (mm^{-1})	143.49
Exposure time (s)	1800
$2\Theta_{min}$ - $2\Theta_{max}$ (°)	12 - 140
R_p; R_{wp}; R_B; GOF	0.0048; 0.0095; 0.0067; 2.07

Table 7. Fractional atomic coordinates and isotropic displacement parameters (B_{iso}, $Å^2$) for selenolaurite

Site	***x***	***y***	***z***	B_{iso}
Ru (4*a*)	0	0	0	1.59(8)
Se (8*c*)	0.3792(2)	= *x*	= *x*	1.86(9)

The EBSD map of the native osmium, selenolaurite and moncheite aggregate from the Ingul placer shows that all selenolaurite grains have the same anhedral morphology (Fig. 8a). The Kikuchi band contrast confirms the high degree of crystallinity of selenolaurite even better than for the Os–Ir alloy (Fig. 8b), all the detached grains are single crystals with no twinning or modularity, as it is visible from the Euler color pattern (Fig. 8c).

https://doi.org/10.1180/mgm.2024.89 Published online by Cambridge University Press

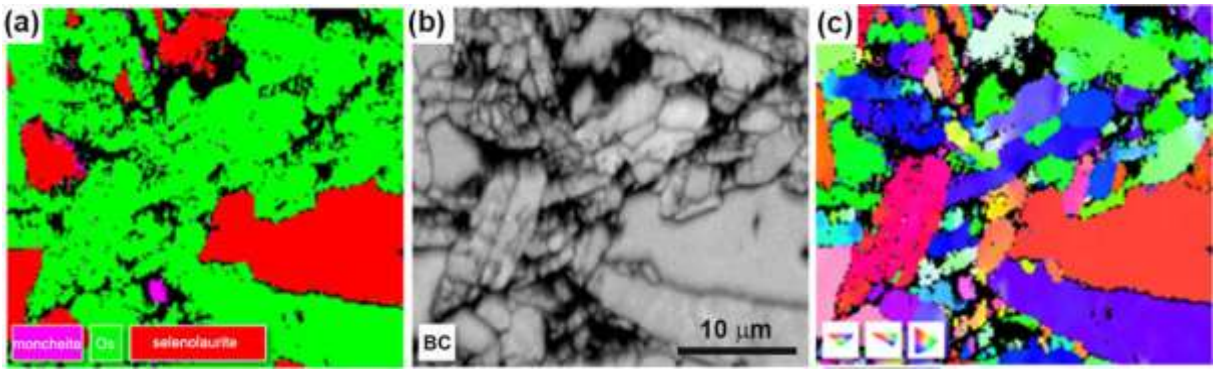

Figure 8. EBSD phase map (a), Kikuchi band contrast (b) and orientation of grains in Euler color (c) of a fragment of the native osmium, selenolaurite and Se-bearing moncheite aggregate.

Discussion

Structure of selenolaurite

Selenolaurite is a Se-dominant analogue of laurite, RuS_2 (Wohler, 1866). Its lattice parameters are close to synthetic $RuSe_2$ (Table 8). The dimension of the lattice of selenolaurite larger than that of laurite is a result of the larger ion size of Se in comparison with S and larger distance Se-Se in comparison with S-S (Lutz et al., 1990).

According to (Zhao et al., 1985), $RuSe_2$ is the only stable phase in the Ru–Se system similarly to RuS_2 for the Ru–S system (Juza and Meyer, 1933).

Table 8. Comparative crystallographic data for selenolaurite, laurite and synthetic $RuSe_2$

Mineral	Selenolaurite	Synthetic	Laurite	Synthetic
Ideal formula	$RuSe_2$	$RuSe_2$	RuS_2	RuS_2
Crystal system	Cubic	Cubic	Cubic	Cubic
Space group	$Pa\bar{3}$	$Pa\bar{3}$	$Pa\bar{3}$	$Pa\bar{3}$
a, Å	5.9424	5.9336	5.6089	5.6106

https://doi.org/10.1180/mgm.2024.89 Published online by Cambridge University Press

V, Å^3	209.84	208.9	176.5	176.6
D_x, g/cm^3	8.42	8.23	6.39	6.21
Reference	This work	Lutz et al. 1990	Bowles et al. 1983	Lutz et al. 1990

Chemical composition of selenolaurite

The limited data available on the composition of selenolaurite and Se-bearing laurite from four known localities indicate the presence of a miscibility gap between laurite and selenolaurite (Fig. 7). This can probably be explained by different ionic radii of Se and S and their ability to form joint S–Se anion dumbbells.

An insignificant Te and Pt content of selenolaurite is due to the presence of moncheite with corresponding elements in the same assemblage. In addition, $RuSe_2$ and $PtSe_2$ do not form a continuous isomorphic series, since PtSe2 (mineral sudovikovite) has a trigonal layered structure, which differs from the pyrite-like structure of selenolaurite.

There is a negative correlation between Ru and Os similar to the full isomorphic miscibility in the laurite–erlichmanite series (Bowles et al., 1983). A similar trend also exists for Ru and Rh, although sulfides with the same Rh:S ratio are unknown. The Ir and Ru contents have a trend of positive correlation, but in the grains from one placer their distribution is not correlate.

Note that, based on the ratio of Ru and other PGEs, the composition of Se-bearing laurite and selenolaurite from various placers form slightly overlapping individual fields and, possibly, characterize specific signatures of individual placers (Fig. 9).

https://doi.org/10.1180/mgm.2024.89 Published online by Cambridge University Press

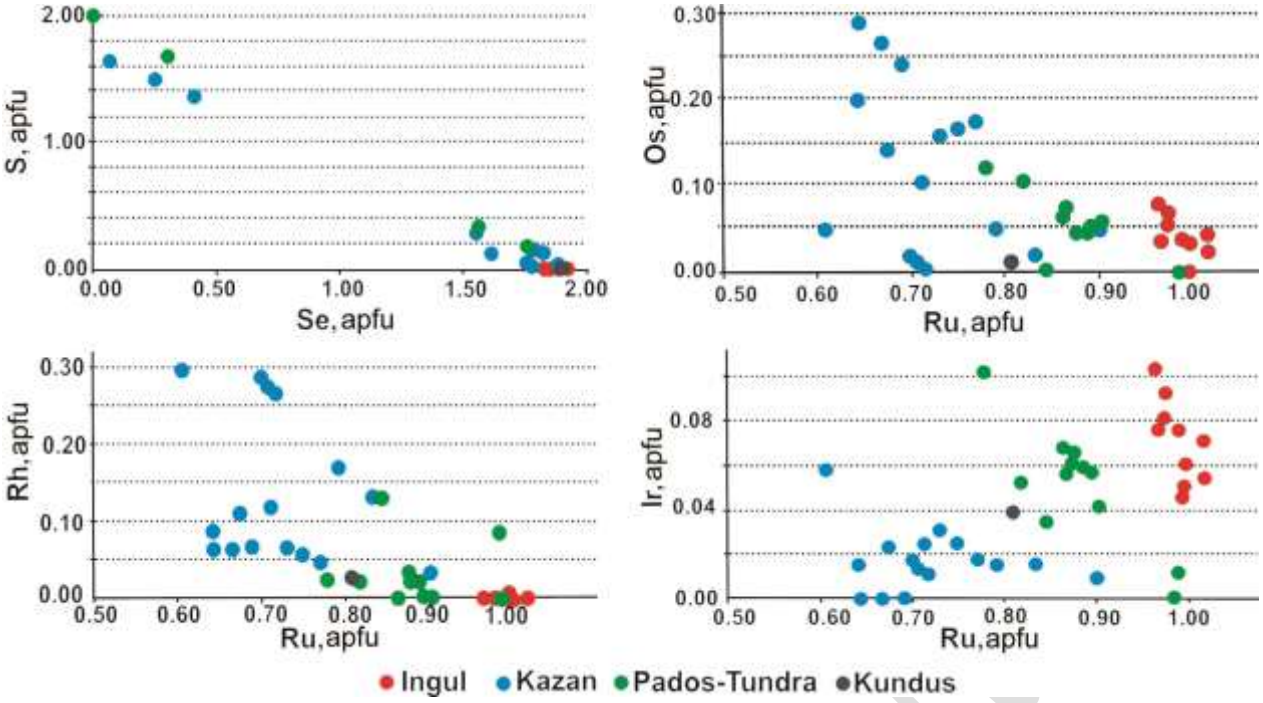

Figure 9. Binary plots characterizing the composition of selenolaurite and Se-bearing laurite.

Source and formation conditions of noble metals minerals in placers

Judging from the present-day topography, native gold of the Ingul placer could be sourced from small gold-bearing silicified zones with quartz veins, which are localized in weakly metamorphosed clay–carbonaceous sedimentary rocks intercalated with Paleozoic volcanic and volcaniclastic rocks of in the East Uralian metallogenic zone. The Kazan placer occurs in the same geological situation, where small uneconomic gold occurrences of various genetic types are supposed to be the sources of native gold (Belogub et al., 2021).

The source of the PGMs of the Ingul placer could be related to small bodies of serpentinized ultramafic rocks of the East Uralian belt of ultramafic and ultramafic-mafic intrusions, which divides the Ilmeny–Vishnevogorsk Terrane and the East Uralian Zone. Selenolaurite and associated moncheite of the Ingul placer form interstitial aggregates between the native osmium crystals and thus are the latest PGMs crystalized after the osmium.

The better studied Nurali ultramaphic massif from the MUF one (Zaccarini et al., 2004) cannot be considered as a source of PGM for the Ingul placer, as the topography contradicts this. The set PGMs in the Maly Iremel placer which is located in close proximity to the Nurali massif

https://doi.org/10.1180/mgm.2024.89 Published online by Cambridge University Press

differs from the mineral composition of PGMs of the Ingul placer by a significant amount of Pt-Fe alloys (Fig. 10). Minerals of the Pt-Fe system, which is typical for PGM of the Ural-Alaskan type massifs (Zakkarini et al., 2018; Stepanov et al. 2020 and reference therein) were not recorded in the Ingul placer as well as in the Kialim placer related with Karabash massif (Rassomakhin et al., 2017). Os-Ir-Ru alloys of the Ingul placer are characterized by a distinct ruthenium trend (Fig. 10), which is more typical for PGM from chromitites of the lower part of the ophiolite section. No minerals of the Pt-Fe are found in the Ingul placer. In several grains of Os-Ir-Ru alloys of Ingul placer, rounded inclusions of high-chromium chromite were found, the composition of which is calculated by the formulas $Mg_{0.668\text{-}0.293}Fe_{0.668\text{-}0.311}Mn_{0.045\text{-}0})(Cr_{1.707\text{-}1.488}Al_{0.508\text{-}0.296}Fe^{3+}{}_{0.036\text{-}0})$ (Zaykov et al., 2018). Chromites of this composition are found both in ultramafites of the mantle part of the ophiolite section and in zonal massifs of the Ural-Alaska type. Unfortunately, ultramafites of potential sources for PGMs of the Ingul placer have not been characterized at the present level.

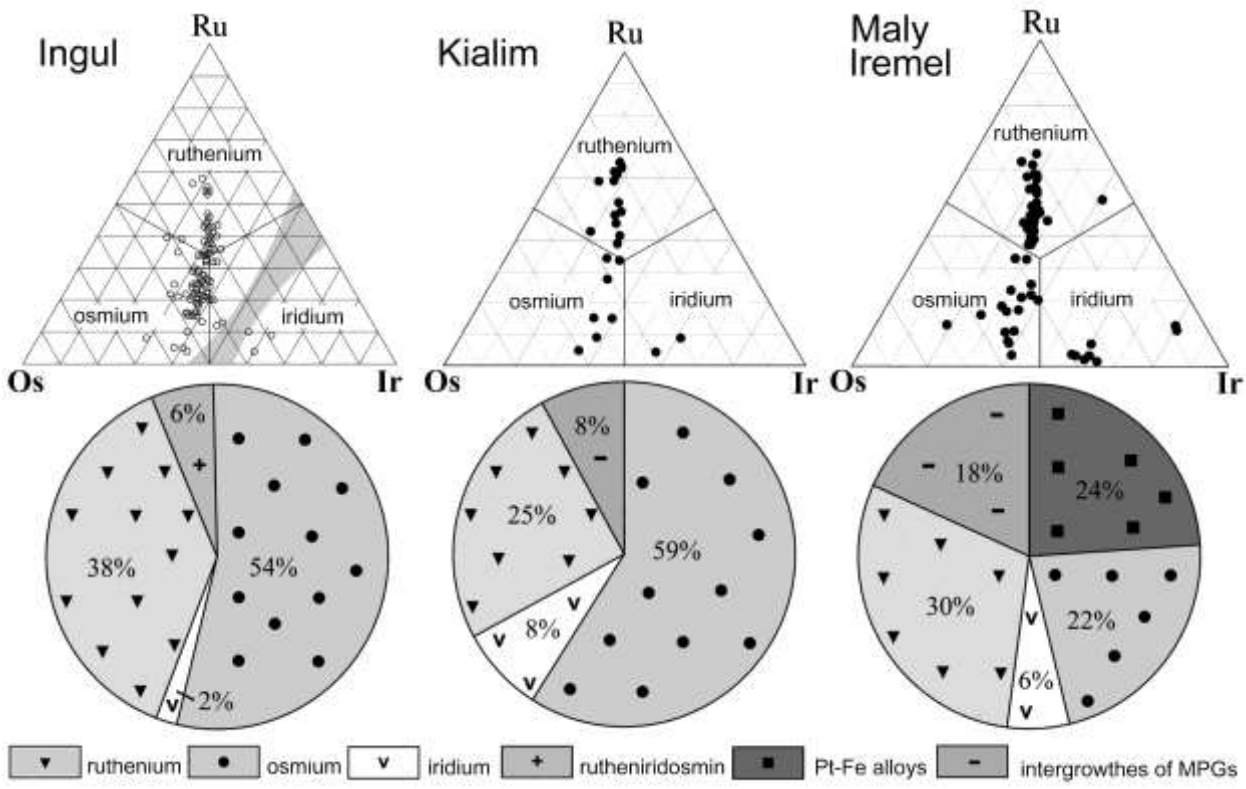

Figure 10. Composition of the Os-Ir-Ru alloys and set om PGMs of the Ingul, Kialim and Maly Iremel placers (Rassomakhin and Zaykov, 2017).

https://doi.org/10.1180/mgm.2024.89 Published online by Cambridge University Press

In a gold-bearing placer of the Kundus River (East Tyva, Russia), selenolaurite was identified as inclusions in native osmium grains. Isoferroplatinum, ferrous and cuprous platinum and its arsenides and tellurides, palladodymite, and minerals of the laurite-erlichmanite series were also described as inclusions in Os–Ir–Ru minerals grains. The ophiolitic serpentinized harzburgites were suggested to be a source of the PGMs for this placer (Oydup et al., 2012).

Two unnamed Se-bearing chalcogenides of Ir and Os occupy a similar position in Os-Ir-Ru grains from placers of the Eastern Russia. Unnamed selenide of Ir and Os with small admixture of Ru replaces Os-Ir-Ru at placer of the Aunik River, Buryatia, Russia. It forms cement of the secondary osmium in the joint inclusion within iridium grains (Airiyants et al., 2020). Unnamed selenoarsenide of Ir and Os from placer of the Kitoy river, West Sayan Ridge, Russia replace osmium during late hydrothermal alteration (Airiyants et al., 2022). The sources of PGMs for both mentioned placers are ophiolitic ultramafic rocks (Airiants et al., 2020, 2021). Selenium-enriched sperrylite was described in the Zolotaya placer, located in the Kartushibinsky ophiolitic belt (Tuva) (Tolstykh et al., 1997).

As pointed by O'Driscoll and González-Jimenéz (2016), approximately 80% of PGMs in placers associated with ophiolites are the Os–Ru–Ir alloys. The general enrichment in refractory PGE and the predominance of Ru members of the laurite-erlichmanite series are characteristic of chromitites of the lower part of the ophiolite section (O'Driscoll and González-Jimenéz, 2016 and reference therein).There is thus a reason to assume that the aggregates of native osmium crystals with selenolaurite in the Ingul placer derived from chromitites of lower part of ophiolite section. Thus, Se-bearing PGMs are more possible in association with ophiolites.

In contrast, Se-bearing laurite and selenolaurite of the Kazan placer form euhedral inclusions in isoferroplatinum grains and are associated with cooperite (Fig. 4). The Gogino zoned gabbro–pyroxenite–dunite massif or Varshavka and Mogutovsky serpentinized dunite–harzburgite massifs were suggested to be a source of the PGMs of the Kazan placer. The genetic type of these massifs is still discussable. The specific feature of the Kazan placer is related to the predominance of isoferroplatinum among the PGMs (Zaykov et al., 2017) and Rh enrichment (Zaykova et al., 2020; Belogub et al., 2021). The Pt-rich character of the PGE spectrum is

https://doi.org/10.1180/mgm.2024.89 Published online by Cambridge University Press

characteristic of the late stage of the formation of the zoned mafic–ultramafic complexes (O'Driscoll and Gonsalez-Jimenes, 2016). Platinum and Rh enrichment relative to chondrite was previously demonstrated for magmatic Ni–(± Cu–± PGE)–sulfide deposits in non-komatiitic rocks (Naldrett, 2004), but sulfides and arsenides are the main PGE mineral forms of mentioned deposits. Moreover, selenium minerals even Se-bearing MPGs were not found in zoned massifs of the Uralian-Alaskian type during a recent study using modern local methods (Stepanov et al., 2020, 2019).

The Se-enriched laurite and an unnamed Se-analogue of laurite from the Pados-Tundra ultramafic complex occur in chromite–magnesiochromite grains in dunite and are associated with chlorite and an an Os-dominant alloy (Barkov et al., 2017). These authors believed that the Se-bearing PGMs formed during autometasomatic alteration of the Pados-Tundra zoned dunite–harzburgite–orthopyroxenite complex.

The ophiolitic and zoned mafic–ultramafic complexes can thus be potential sources of Se-enriched laurite and selenolaurite. In all mentioned cases, these minerals could form at highly S-deficient conditions at a low S fugacity. The coexistence of a low-Os variety of laurite with Os-dominant alloys at the Pados-Tundra complex took place probably below the Os–OsS_2 buffer (Barkov et al., 2017). These conditions could occur at the late stage of the formation of mafic–ultramafic complexes. It is likely that the low S fugacity and a sufficient Se amount led to the formation of the described rare Ru selenide.

Conclusion

A new ruthenium selenide selenolaurite, ideally $RuSe_2$, is described as a matrix of an aggregate of the Os–Ir–Ru alloy together with moncheite $PtTe_2$ in a heavy concentrate of the Ingul gold placer, South Urals, Russia. The structural features of selenolaurite indicate its later formation compared to the Os–Ir–Ru alloy.

https://doi.org/10.1180/mgm.2024.89 Published online by Cambridge University Press

Selenolaurite is a selenium analogue of laurite with a pyrite crystal structure. According to available empirical data, there is a miscibility gap of the laurite–selenolaurite series because of geometrical difference between S_2^{2-} and Se_2^{2-}.

The surface topography and the characteristics of rocks drained by the Ingul River support the assumption that the ultramafic rocks exposed by the Chebarkul–Katsbakh deep fault in the eastern frame of the Ilmeny–Vishnevogorsk magmatic–metamorphic complex are the PGM source for the Ingul placer.

To date, four findings of the ruthenium selenide are described, including three in PGM-bearing gold placers and one in lode chromitites from a zonal mafic–ultramafic intrusion. In the Ingul and Kundus placers, selenolaurite was found in assemblage with Os–Ir–Ru alloys, the composition of which is statistically characterized by elevated Ru concentrations. No Pt–Fe alloys were found in these placers and Pt occurs as chalcogenides only. These features are typical of the PGM assemblages from chromitites associated with mantle part of ophiolite sections.

In the Kazan placer, selenolaurite is found as euhedral inclusions in Pt_3Fe. In primary chromitites of the Pados–Tundra zonal complex, selenolaurite forms euhedral inclusions associated with Os and RhTe compound in chromite. By analogy with widespread euhedral inclusions of laurite in chromite and isoferroplatinum, the origin of selenolaurite in these cases can be interpreted as late magmatic also.

It is thus supposed that selenolaurite forms during the late magmatic stage in different types of ultramafic rocks at highly S-deficient conditions, low S fugacity and high Se fugacity.

The reason of the Se enrichment of some ophiolite-related placers remains still unclear.

Acknowledgments: The authors are grateful to N.P. Zemlyanskiy (Ingul Cooperative) and A.Yu. Ivanov and B.Ya. Hismatullin (Miass Priisk Company) for heavy concentrates from the Ingul and Kazan placers, respectively, and M. Lozhkin (Nanophotonics Resource Center, SPSU) for the preparation of the sample surface for EBSD mapping. This work was supported by state contract no. 122031600292-6. The authors acknowledge Saint-Petersburg State University Research

https://doi.org/10.1180/mgm.2024.89 Published online by Cambridge University Press

Project no. 116234388 supporting the EBSD study. The authors are thankful to the reviewers Anna Vymazalová and Federica Zaccarini whose comments helped improve the article.

Conflicts of Interest: The authors declare no conflict of interest.

References

Airiyants, E.V.; Kiseleva, O.N.; Zhmodik, S.M.; Belyanin, D.K.; Ochirov, Y.C. (2022) Platinum-Group Minerals in the Placer of the Kitoy River, East Sayan, Russia. Minerals 2022, 12, 21. https://doi.org/10.3390/ min12010021

Airiyanys E. V., Belyanin, D. K., Zhmodik, S. M., Agafonov, L. V., & Romashkin, P. A. (2020). Chemical composition and origin of platinum-group minerals from placers of the Aunik River, Buryatia, Russia. Ore Geology Reviews, 120, 103453.

Barkov A. Y., Nikiforov A. A., Tolstykh N. D., Shvedov G. I., Korolyuk V. N. (2017) Compounds of Ru-Se-S, alloys of Os-Ir, framboidal Ru nanophases, and laurite-clinochlore intergrowths in the Pados-Tundra complex, Kola Peninsula, Russia. European Journal of Mineralogy, 29, 613-621

Barkov, A.Y.; Nikulin, I.I.; Nikiforov, A.A.; Lobastov, B.M.; Silyanov, S.A.; Martin, R.F. Atypical Mineralization Involving Pd-Pt, Au-Ag, REE, Y, Zr, Th, U, and Cl-F in the Oktyabrsky Deposit, Norilsk Complex, Russia. Minerals 2021, 11,1193. https://doi.org/10.3390/min11111193

Belogub E.V., Britvin S.N., Shilovskikh V.V., Pautov L.A., Kotlyarov V.A., Zaykova E.V. Zaykovite, Rh3Se4, a new mineral from the Kazan placer, South Urals, Russia // Mineralogical Magazine. 2023, 87(1), страницы 118–129 DOI: 10.1180/mgm.2022.122

Belogub, E.V., Zaykova E.V., Kotlyarov V.A., Shilovskikh V.V., Britvin S.N. and Pautov L.A. 2019) Selenium in the minerals of the platinum group minerals from gold placer of the South Urals. Mineralogical museums: Conference material. Sain-Petersburg, SPbU. 87-89. [In Russian].

Bowles J. F. W., Atkin D., Lambert L. M., Deans T., Phillips R. (1983) The chemistry, reflectance, and cell size of the erlichmanite (OsS2) – laurite series. Mineralogical Magazine, 47, 465-471.

Cabri L. J., Oberthür, T., and Keays, R. (2022) Origin and depositional history of platinum-group minerals in placers – A critical review of facts and fiction, Ore Geol. Rev., 144,104733, https://doi.org/10.1016/j.oregeorev.2022.104733

Clarke M.J. (2003) Ruthenium metallopharmaceuticals. Coordination Chemistry Reviews 236: 209-233

Cook N. J., Wood S. A., Gebert W., Bernhardt H. J. and Medenbach, O. (1994) Crerarite, a new Pt-Bi-Pb-S mineral from the Cu-Ni-PGE deposit at Lac Sheen, Abitibi-Temiscaminque, Quebec, Canada. Neues Jahrbuch für Mineralogie, Monatshefte, 567-575.

Davis R.J., Clark A.M. and Criddle A.J. (1977) Palladseite, a new mineral from ltabira, Minas Gerais, Brazil. Mineralogical Magazine, 41, 123.

Greenwood N.N. and Earnshaw A. (1997) Iron, Ruthenium and Osmium in Chemistry of the Elements. Second edition Reed Educational and Professional Publishing Ltd, 1997. Pp. 1070-1112

Jebwab J., Cervelle B., Gouet G., Hubaut X. and Piret P. (1992) The new platinum selenide luberoite Pt5Se4 from the Lubero region (Kivu Province, Zaire). European Journal of Mineralogy, 4, 683-692.

Johan Z., Picot P. and Pierrot R. (1970) L'oosterboschite (Pd,Cu)7Se5, une nouvelle espèce minérale et la trogtalite cupro-palladifère de Musonoï (Katanga). Bulletin de la Société française de Minéralogie et de Cristallographie, 93, 476-481.

Juza R. and Meyer W. (1933) Beiträge zur systematischen Verwandtschaftslehre. 59. Über die Sulfide des Rutheniums. Z. Anorg. Allg. Chem. 213(3) 273-282

Ivanischev A.V., Sazonov V.N., Savelieva K.P. et al. (2005) Systematics and sorting of a gold deposits of the Sverdlovsk and Chelyabinsk districts, that were exploited at the former years

https://doi.org/10.1180/mgm.2024.89 Published online by Cambridge University Press

targeted to estimation their perspectives. Uralnedra, South-Ural geological center LTd. [in Russian].

Krivovichev V.G. Mineral species (2021). St.Petersburg Univ. Publ. House. 599 pp. [In Russian].

Leonard B.F., Desborough G.A. Ore microscopy and chemical composition of some laurites // American Mineralogist 54. 1969. 1330-1346

Lorand J.-P. and Luguet A. (2016) Chalcophile and Siderophile Elements in Mantle Rocks: Trace Elements Controlled By Trace Minerals / Reviews in Mineralogy & Geochemistry Vol. 81 pp. 441-488 http://dx.doi.org/10.2138/rmg.2016.81.08

Lutz H. D., Müller B., Schmidt T., Stingl T. (1990) Structure refinement of pyrite-type ruthenium disulfide RuS2 and ruthenium diselenide, RuSe2. Acta Crystallographica, C46, 2003-2005

Mason J., Schuh C. (2009) Representations of texture, in Electron Backscatter Diffraction in Materials Science (in Schwartz, A.J., Kumar, M., Adams, B.L., Field, D.P eds.), Springer, 35-51.

Naldrett, A. (2004). Magmatic sulphide deposits – Geology, geochemistry and exploration. Springer-Verlag, Berlin, p. 728

O'Driscoll B., González-Jiménez J.M. Petrogenesis of the Platinum-Group Minerals / Reviews in Mineralogy & Geochemistry, Vol. 81 pp. 489-578, 2016 http://dx.doi.org/10.2138/rmg.2016.81.09

Oydup Ch.K., Mongush A.A., Khuragan Ch.M. (2012) Typomorphic features of the minerals of platinum group in the Kundus gold placer (KaaKhem ophiolitic belt, Tyva). Russial lithology and raw materials, 5, 490–498. [In Russian]

Paar W.H., Roberts A.C., Criddle A.J. and Topa D. (1998) A new mineral, chrisstanleyite, Ag2Pd3Se4, from Hope's Nose, Torquay, Devon, England. Mineralogical Magazine, 62(2), 257–264

https://doi.org/10.1180/mgm.2024.89 Published online by Cambridge University Press

Polekhovskiy Y.S., Tarasova I.P., Nesterov A.P., Pakhomovskiy Y.A. and Bakhchisaraitsev A.Y. (1997) Sudovikovite PtSe2 - a new platinum selenide from Karelia metasomite. Doklady Akademii Nauk, 354, 82-85. [In Russian]

Rassomakhin M.A., Zaykov V.V. (2017) Composition of the platinoids of Ingul Placer (South Urals). Metallogeny of the ancient and modern oceans – 2017. V.1, 119-123. [In Russian]

Reith, F., Zammit, C.-M., Shar, S.S., Etschmann, B., Bottrill, R., Southam, G., Ta, C., Kilburn, M., Oberthür, T., Ball, A.S., 2016. Biological role in the transformation of platinum-group-mineral grains. Nat. Geosci. 9, 294–298.

Roberts W. L., Campbell T., Rapp G.R. Jr. (1990) *Encyclopedia of Minerals*, 2th edition. Van Nostrand Reinhold Co., New York.

Roberts A.C., Paar, W.H., Cooper, M.A., Topa, D., Criddle, A.J. and Jedwab, J. (2002) Verbeekite, monoclinic PdSe2, a new mineral from the Musonoi Cu-Co-Mn-U mine, near Kolwezi, Shaba Province, Democratic Republic of Congo. Mineralogical Magazine, 66, 173-179.

Stepanov, S.Yu., Palamarchuk, R.S., Antonov, A.V., Kozlov, A.V., Varlamov, D.A., Khanin, D.A., Zolotarev Jr., A.A. (2020). Morphology, Composition, and Ontogenesis of Platinum-group minerals in chromitites of zoned clinopyroxenite-dunite massifs of the Middle Urals. Russ. Geol. Geophys. 61, 47–67. https://doi.org/10.15372/ RGG2019089.

Stepanov, S.Yu., Palamarchuk, R.S., Kozlov, A.V., Khanin, D.A., Varlamov, D.A., Kiseleva, D.V. (2019). Platinum-group minerals of Pt-placer deposits associated with the Svetloborsky Uralian-Alaskan type massif, Middle Urals, Russia. Minerals 9, 77.

Sutarno, O. K, Reid K.I.G. (1967) Chalcogenides of the transition elements. V. Crystal structures of the disulfides and ditellurides of ruthenium and osmium Canadian Journal of Chemistry, v.45(12) 1391-1400 doi.org/10.1139/v67-230

The quantitative data file for ore minerals (1986). A.J.Criddle and C.J.Stanley editors. Comission on ore microscopy of the International Mineralogical association. British museum (Natural history), 1986, 420 pp

https://doi.org/10.1180/mgm.2024.89 Published online by Cambridge University Press

Tolstykh, N.D., Krivenko, A.P., Pospelova, L.N. (1997): Unusual compounds of iridium, osmium, and ruthenium with selenium, tellurium and arsenic from the placers of the Zolotaya River (western Sayan). Zap. Vseross. Mineral. Obshch (ZVMO): 126(6): 23–34 (in Russian);

Vymazalová A., Laufek F., Drábek M., Cabral A.R. Haloda J., Sidorinová T., Lehmann B., Galbiatti H.F. and Drahokoupil J. (2012) Jacutingaite, Pt2HgSe3, a new platinum-group mineral species from the Cauê iron-ore deposit, Itabira district, Minas Gerais, Brazil. Canadian Mineralogist, 50(2), 431-440.

Wöhler, F. (1866) Ueber ein neues mineral von Bornéo. Nachrichten von der Königliche Gesellschaft der Wissenschaftern und der Georg-Augusts-Universität: 1866: 155-160.

Zaccarini F., Pushkarev E., Fershtater G., Garuti G. (2004) Composition and mineralogy of PGE-rich chromitites in the Nurali lherzolite gabbro complex, Southern Urals, Russia. The Canadian Mineralogist, 42(2), 545-562.https://doi.org/10.2113/gscanmin.42.2.545.

Zaccarini F., Garuti G., Pushkarev E., Thalhammer O. (2018) Origin of platinum group minerals (PGM) inclusions in chromite deposits of the Urals. Minerals, 2018, 8, 379, doi:10.3390/min8090379

Zaccarini F, Economou-Eliopoulos M., Kiseleva O., Garuti G., Tsikouras B., Pushkarev E., Idrus A. (2022) Platinum Group Elements (PGE) Geochemistry and mineralogy of low economic potential (Rh-Pt-Pd)-rich chromitites from ophiolite complexes. Minerals, 12, 1565. https://doi.org/10.3390/min12121565

Zaykov V. V. Melekestseva I. Yu., Zaykova E. V., Kotlyarov V. A., Kraynev Yu. D. (2017) Gold and platinum group minerals in placers of the South Urals: Composition, microinclusions of ore minerals and primary sources. Ore geology reviews, 85, 299-320.

Zaykov V.V., Zaykova E.V., Blinov I.A., Oydup Ch.K., Mongush A.A. (2014) Platinoids from the gold placer of Kundus river (Tuva) Materials of the Urals mineralogical school – 2014, 69-76.

https://doi.org/10.1180/mgm.2024.89 Published online by Cambridge University Press

Zaykova E.V., Blinov I.A., Kotlyarov V.A. (2020) MINERAL INCLUSIONS IN PLATINUM GRAINS FROM THE KAZAN PLACER (SOUTH URALS). Mineralogy 6(1) DOI: 10.35597/2313-545X-2020-6-1-3.

Zhao H. Schils H.W. Raub Ch.J. (1985) Untersuchungen im system ruthenium-selen-tellur. Journal of the Less Common Metals 113(1), 75-82.

https://doi.org/10.1180/mgm.2024.89 Published online by Cambridge University Press